

Evaluation of PCM/diatomite composites using exfoliated graphite nanoplatelets (xGnP) to improve thermal properties

Su-Gwang Jeong · Jisoo Jeon · Okyoung Chung ·
Sughwan Kim · Sumin Kim

Received: 24 October 2012 / Accepted: 21 January 2013 / Published online: 2 March 2013
© Akadémiai Kiadó, Budapest, Hungary 2013

Abstract This paper deals with the thermal performances of shape-stabilized phase change materials (SSPCM) for energy saving in various fields. This study enhanced thermal properties of SSPCM using exfoliated graphite nanoplatelets (xGnP). SSPCM, which contains the xGnP, was prepared by mixing and melting techniques for high dispersibility, thermal conductivity, and latent heat storage. In the experiment, we used hexadecane, octadecane, and paraffin as phase change materials (PCMs), and they have 254.7, 247.6, and 144.6 J g⁻¹ of latent heat capacity, and melting points of 20.84, 30.4, and 57.09 °C, respectively. The characteristics of SSPCMs were determined using SEM, DSC, FTIR, TG, TCI, and Energy simulation. SEM morphology showed homogenous dispersion of PCM and xGnP in the porous diatomite. DSC analysis results showed the latent heat capacity of SSPCM and SSPCM/xGnP composites, and TG analysis results showed the thermal reliability of the samples. Also, we checked the thermal conductivity of the SSPCM that contains xGnP, by TCI analysis.

Keywords PCM · Diatomite · Heat storage · Impregnation · Thermal conductivity · xGnP · Energy simulation

Introduction

Energy needs for a wide variety of applications mainly depend on the time and energy resources available.

Therefore, energy storage is often required to meet various demands for energy. Among the different methods of thermal energy storage, latent energy storage has become one of the most attractive techniques [1]. Excess thermal energy is stored in a material as latent heat, by melting the material. The stored thermal energy is utilized later, when necessary, by freezing the material again. Solar energy is a renewable energy, and hence the need for fossil fuels and green house gas emissions can be reduced. Thus, these systems have potential applications in active and passive solar heating, water heating, air conditioning, etc., and are regarded as an economical and safe energy storage technology. Solar energy can effectively be stored during the day, and thereafter, it can be used at a later stage [2].

In recent times, several inorganic and organic PCMs and their mixtures have been studied as candidate PCMs for latent heat thermal energy storage applications [3]. However, the application of PCMs in various fields is difficult, due to their phase instability in the liquid state. Therefore, PCMs need shape stabilization. There are many studies that have tried to solve leakage and improve the thermal conductivity properties of PCM. In order to solve the leakage of PCM during the phase change, conventional methods, including encapsulation and physical mixing technologies, have been investigated [4]. In recent years, a new type of PCM called shape-stabilized PCM (SSPCM), composed of PCM and supporting materials, has been developed. Different PCMs should have congruent supporting materials. If the PCM is based on organic matter, the supporting material should have a similar skeleton, such as high-density polyethylene (HDPE), polypropylene (PP), and styrene-butadiene-styrene (SBS). Many studies on SSPCMs had been carried out. Xu et al. developed a new kind of SSPCM plate which consists of 70 wt% paraffin as the dispersed PCM, and 15 wt% polyethylene and 15 wt% SBS block copolymer as

S.-G. Jeong · J. Jeon · O. Chung · S. Kim · S. Kim (✉)
Building Environment and Materials Lab, School of
Architecture, Soongsil University, Seoul 156-743, Korea
e-mail: skim@ssu.ac.kr

the supporting materials. The thermal and physical properties of the developed SSPCM were evaluated for application as a walling product [5]. Lin et al. developed SSPCM plates which consist of 75 wt% paraffin as a dispersed PCM, and 25 wt% polyethylene as a supporting material. This SSPCM system can be used for heat storage using cheap nighttime electricity and discharging the heat stored during the daytime [6]. Zhang et al. developed an SSPCM consisting of paraffin with a melting point of 20 or 60 °C as a PCM, and HDPE or a composite as supporting material [7]. Cheng et al. reported that the thermal conductivity of shape-stabilized paraffin/HDPE composite PCM was improved by the addition of graphite powder and expanded graphite [8]. Alkan et al. described the preparation of MPCMs by coating n-eicosane with PMMA shell, to improve the thermal properties and thermal reliability [9]. Diatomite has light mass, high porosity, high absorptivity, high purity, multi-shape, rigidity, and inertness. Both the chemical composition and the physical structure of diatomite make it suitable for many scientific and industrial purposes. Diatomite is used in many fields as a filtering agent; building material; heat, cold, and sound insulator; catalyst carrier; filler absorbent; abrasive; and ingredient in medicines [10]. Considering all that is mentioned above, diatomite is one of the feasible candidates as an economical and light mass building material, for incorporating PCM for thermal energy storage in buildings.

PCMs that are used as storage media in latent thermal energy storage can be classified into two major categories: organic and inorganic compounds. Inorganic PCMs include salt hydrates, salts, metals and alloys, whereas organic PCMs comprise hexadecane, octadecane, paraffin, and fatty acids/esters etc. Organic PCMs would be useful for application in various fields as a PCM, because it has a large latent heat and low cost, and is stable, non-toxic, and noncorrosive [11, 12]. However, the main drawback that hinders the application of organic PCMs is their unacceptably low thermal conductivity. Great efforts, such as improving the encapsulation structure, dispersing high conductive fillers in organic PCMs matrixes [13–17], and dispersing organic PCMs in high conductive matrixes [18, 19], have been devoted to improve the thermal conductivity of organic PCMs. However, few organic PCMs have attained satisfactory thermal conductivity while maintaining reasonable thermal energy storage density. Mills et al. [20] improved the thermal conductivity of paraffin by impregnating porous graphite matrix with paraffin. Also Zeng et al. [21] improved the thermal conductivity of organic PCMs using Ag nano wires. Kim et al. [3] studied the effect of exfoliated graphite nano platelets addition on the thermal properties of the paraffin wax/xGnP composite prepared as a form-stable PCM, and reported that the thermal conductivity of PCM increased with increasing graphite mass fraction. Therefore, we studied PCM/diatomite composite with xGnP to improve thermal conductivity

for energy saving. This study also aims to investigate the effect of the xGnP addition on the dispersibility, thermal conductivity, and latent heat capacity of SSPCM [22].

Experimental

Materials

This study used three types of liquid organic PCMs with different melting points. In the experiment, we used hexadecane, octadecane, and paraffin as PCMs, which have 254.7, 247.6, and 144.6 J g⁻¹ of latent heat capacity, and melting points of 20.84, 30.4, and 57.09 °C, respectively. The PCMs were obtained from Celsius Korea company in South Korea, and the diatomite sample was supplied from Samyoung Global Corporation in South Korea. The diatomite sample has a diameter below 10 μm, and was dried at 105 °C for 24 h before use. Exfoliated graphite nanoplatelets (xGnP) are prepared from sulfuric acid-intercalated expandable graphite (3772), obtained from Asbury Graphite Mills, NJ, by applying a cost and time effective exfoliation process initially proposed by Drzal's group [3].

Preparation

The SSPCM was prepared using a vacuum impregnation method [23, 24]. The 5 wt% of xGnP, according to mass percentage of diatomite, was mixed in diatomite before the vacuum process. The xGnP/diatomite mixture was placed inside a filtering flask which was connected to a water trap apparatus, to evacuate air from its porous surface. Then, the valve between the flask and the container of 80 g of liquid PCM was turned open to allow it to flow into the flask, to cover the xGnP/diatomite mixture. After the vacuum process was continued for 90 min, air was allowed to enter the flask again, to force the liquid PCM to penetrate into the pore space of the xGnP/diatomite mixture. To find the maximum PCM amount in the xGnP/diatomite mixture, we impregnated 80 g of PCM into the xGnP/diatomite mixture. In this case, no impregnated excess of PCM remained in the flask. Therefore, we needed to remove the excess of PCM in the flask through filtering. The colloid state of SSPCM was filtered by 1 μm filter paper, until a granule type of sample appears on the filter paper. Then the granule type of SSPCM was dried in a vacuum drier at 80 °C for 24, 48, and 72 h, for each PCM (hexadecane, octadecane, paraffin).

Characterization techniques

To confirm the characteristics of SSPCM, we carried out scanning electron microscopy (SEM, JEOL JSM-6360A),

Fourier transform infrared spectroscopy (FTIR), differential scanning calorimetry (DSC), and thermo gravimetric (TG) analysis measurements. The morphology and composition of the SSPCM composites as three types of PCM were observed by means of scanning electron microscopy at room temperature. An SEM with an accelerating voltage of 12 kV and working distance of 12 mm was used to collect the SEM images. The samples were coated with a gold coating of a few nanometers in thickness [3]. FTIR spectroscopy (300E Jasco) was also utilized to monitor the change of chemical groups upon curing. Clear potassium bromide (KBr) disks were molded from the powder, and a pure KBr disk was used as the background. The samples were analyzed over the range of 525–4,000 cm^{-1} , with a spectrum resolution of 4 cm^{-1} . All spectra were averaged over 32 scans. This analysis of the composites was performed at point-to-point contact with a pressure device [25]. Thermal properties, such as the melting temperature and latent heat capacity of pure PCMs and composite PCMs, were measured using a DSC instrument (DSC Q 1000). The melting temperature was measured by drawing a line at the point of maximum slope of the leading edge of the peak, and extrapolating to the base line [26]. The latent heat of the PCM/diatomite was determined as the total by numerical integration of the area under the peaks that represent the solid–solid and solid–liquid phase transitions. Thermo gravimetric analysis measurements of the PCM/diatomite composites were carried out using a TG analyzer (TA Instruments, TGA Q5000) on about approximately 2–4 mg samples over the temperature range, 25–600 °C, at a heating rate of 10 °C min^{-1} , under a nitrogen flow of 20 ml min^{-1} . TG was measured with the composites placed in a high quality nitrogen (99.5 % nitrogen, 0.5 % oxygen content) atmosphere to prevent unwanted oxidation. The thermal conductivity of SSPCM was measured using a TCi thermal conductivity analyzer. The TCi developed by C-Therm Technologies Ltd. is a device for conveniently measuring the thermal conductivity of a small sample, using the Modified Transient Plane Source (MTPS) method [27]. Contrary to other devices, TCi can measure the thermal conductivity of materials in solid, liquid, powder, and mixed states. The TCi consists of a sensor, power control device, and computer software. A spiral-type heating source is located at the center of the sensor, and heat is generated at the center. The heat that has been generated enters the material through the sensor, during which a voltage decrease occurs rapidly at the heating source, and the thermal conductivity is calculated through the voltage decrease data. Simulation has been performed by Energy Plus 6.0. The basic algorithm used in Energy Plus for calculating surface heat transfer is the conduction transfer function (CTF). This describes the transient conduction process with time series coefficients in an algebraic equation. While the CTF solution has the advantage of single and relatively simple linear

equations with constant coefficients, the constant coefficient works as a disadvantage because it is not possible to simulate temperature-dependent thermal properties. In Energy Plus, this has been done by selecting a new solution algorithm, the finite difference method (FDM).

Results and discussion

Morphological analysis of SSPCM

Figure 1 shows the morphology of the SSPCM, and thermal enhanced SSPCM which contains 5 wt% of xGnP particles. The powder type of diatomite has changed to granule type through the PCM impregnating process. From the morphology analysis, each PCM fully filled the diatomite pores. Each SSPCM has a little different morphology because the different PCMs were immersed into the pore space of the diatomite. We analyzed that the thermal enhanced SSPCM, which contains the xGnP, has form stable performance because the surrounding paper was not wet, despite SSPCM being loaded onto the paper. That is, the xGnP does not affect form stabilization of the SSPCM. Also, because the xGnP has loaded onto SSPCM, a black color appears on the samples. This shows that the xGnP dispersed comparatively well into the structure of each SSPCM.

Microstructure SSPCM

Figure 2 shows the SEM analysis of SSPCM with xGnP. Each PCM was completely incorporated well into the porous part of the diatomite. Figure 2a shows SEM micrographs of hexadecane/diatomite composite with xGnP. We found that some nano particles of xGnP were shown in the sample. Because the diatomite has a porous structure for incorporating the PCM, the xGnP and PCMs are well incorporated into the diatomite. Also, we found the same trend from the octadecane/diatomite/xGnP and paraffin/diatomite/xGnP composites, shown in Figs. 2b, c. The xGnP in the SSPCM could enhance thermal conductivity of SSPCM. We also determined that the xGnP has no effect on the incorporating process of PCMs. Therefore, heat storage of PCM is maintained in the SSPCM in spite of loading the xGnP.

FTIR analysis of SSPCM/xGnP Composites

The FTIR absorption spectra of the SSPCM/xGnP composites are shown in Fig. 3. The hexadecane, octadecane, and paraffin are composed of $-\text{CH}_2$ bonding and $-\text{CH}_3$ bonding. Thus, all the FTIR absorption spectra of PCMs are similar. These FTIR absorption spectra are shown from

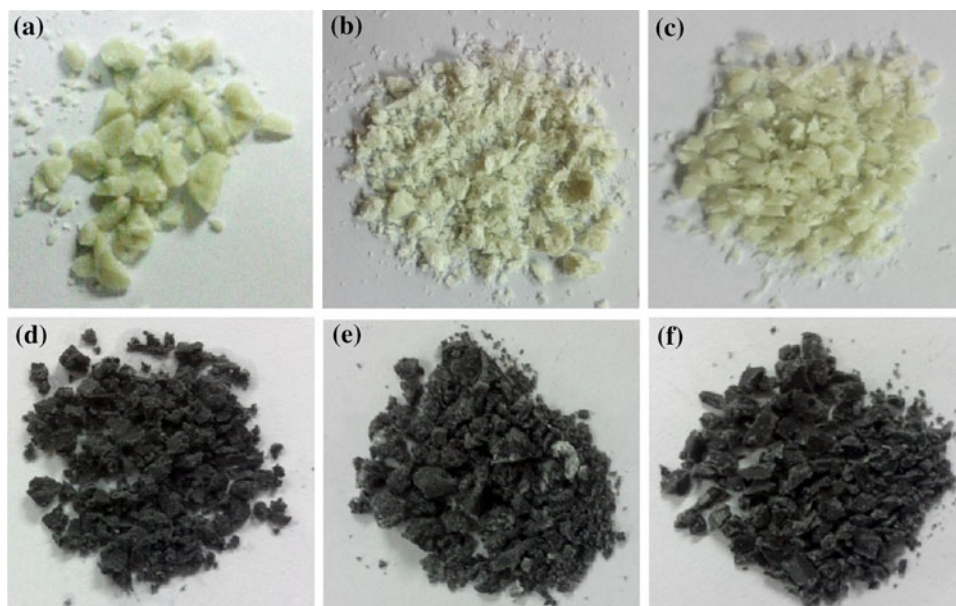


Fig. 1 Sample images of SSPCM and SSPCM with xGnP: **a** Hexadecane+diatomite composite. **b** Octadecane+diatomite composite. **c** Paraffin+diatomite composite. **d** Hexadecane+diatomite+xGnP composite. **e** Octadecane+diatomite+xGnP composite. **f** Paraffin+diatomite+xGnP composite **a–c** PCM + diatomite composites, and **d–f** PCM + diatomite + xGnP composites

2,918, 2,850, 1,468, and 720 cm^{-1} of wave numbers, caused by stretching vibration of functional groups of $-\text{CH}_2$ and $-\text{CH}_3$. Also, diatomite has 1,085, 944, 802, 464 cm^{-1} FTIR peaks. These peaks of PCMs and diatomite were not changed during the incorporating process. This shows that SSPCM is composed of PCM and diatomite by physical interaction. In this experiment, we contained the xGnP to the PCM/diatomite composite. We confirmed that the xGnP has no strong peak from FTIR analysis. Also, the physical bonding between PCM and diatomite is not affected by the containing xGnP. Consequently, we determined that the heat storage characteristics of PCMs remained, after the incorporating process and containment of xGnP.

Heat storage properties of SSPCM/xGnP composites

The heating and freezing curves from the DSC measurements of the SSPCM with xGnP are presented in Fig. 4. In this analysis, we found that the latent heat capacity of SSPCM with xGnP shows the same trend, when compared with PCM/diatomite composite. All PCM/diatomite/xGnP composites showed a similar phase transition range, compared with its pure PCM. The values for thermal performances of the PCM/diatomite composites were nearly 50 % of those of the pure PCMs. Therefore, in the case of the hexadecane/diatomite/xGnP composite, its latent heat capacity is 120.8 and 120.1 J g^{-1} during the

heating and freezing processes, and it is seen in Fig. 4a. Also, in the case of octadecane/diatomite/xGnP composite from Fig. 4b, its latent heat capacity is 126.1 and 112.7 J g^{-1} during heating and freezing. This could be explained in that the containing xGnP does not affect the heat capacity of PCM during the incorporating process. Also, the paraffin group shows approximately 45 % of the heat storage characteristic compared with pure paraffin. Its latent heat capacity is 63.77 and 62.83 J g^{-1} , respectively. We found that the latent heat capacity of SSPCM with xGnP is a little higher than that of SSPCM without xGnP. It seems that a little PCM was incorporated into the porous part of the xGnP. Therefore, it shows that the containing xGnP helps to get more latent heat capacity. However, the difference of heat capacity is very small. Also the melting point of the hexadecane-based SSPCM with xGnP shifted to $22.09\text{ }^\circ\text{C}$ from $23.68\text{ }^\circ\text{C}$ for the SSPCM without xGnP. On the contrary, the freezing point of composite shifted to $13.17\text{ }^\circ\text{C}$ from $17.14\text{ }^\circ\text{C}$ for the pure SSPCM without xGnP [28]. It shows that xGnP leads to prevent the supercooling of SSPCM because xGnP helped the PCMs to absorb and to release heat easily. And the other SSPCMs with xGnP show the same trend. It is verified that the xGnP in the SSPCM brings high thermal efficiency. Therefore, as a result, we expected that this high latent heat capacity of PCM/diatomite/xGnP composite has an important potential for heating and cooling applications in buildings.

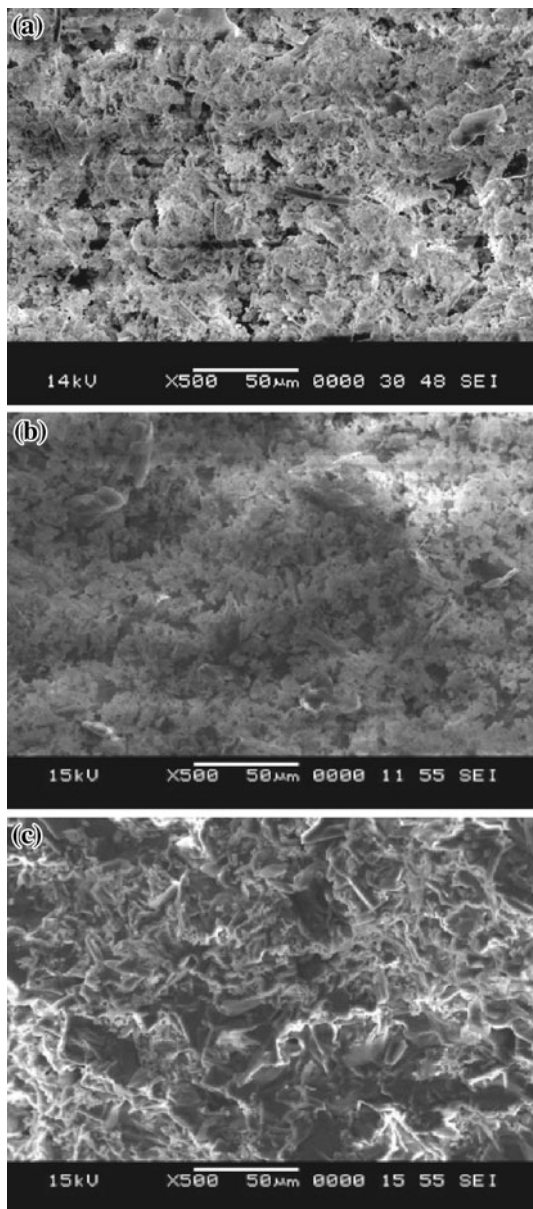


Fig. 2 SEM images of SSPCM + xGnP composites **a** hexadecane + diatomite + xGnP composite, **b** octadecane + diatomite + xGnP composite, and **c** paraffin + diatomite + xGnP composite

Thermal resistance analysis

Since diatomite and xGnP are known for their resistance to thermal degradation, thermal decomposition of the PCM/diatomite/xGnP composites was analyzed by TG in a nitrogen atmosphere, as shown in Fig. 5. All the degradation peaks have one curve by the PCMs thermal oxidation degradation. Also, SSPCM with xGnP occurred with 50 % thermal degradation of mass, similar to SSPCM without xGnP. We found that the TG peak of SSPCM with xGnP occurred with thermal degradation late in time, compared with SSPCM without xGnP. It shows that the containing

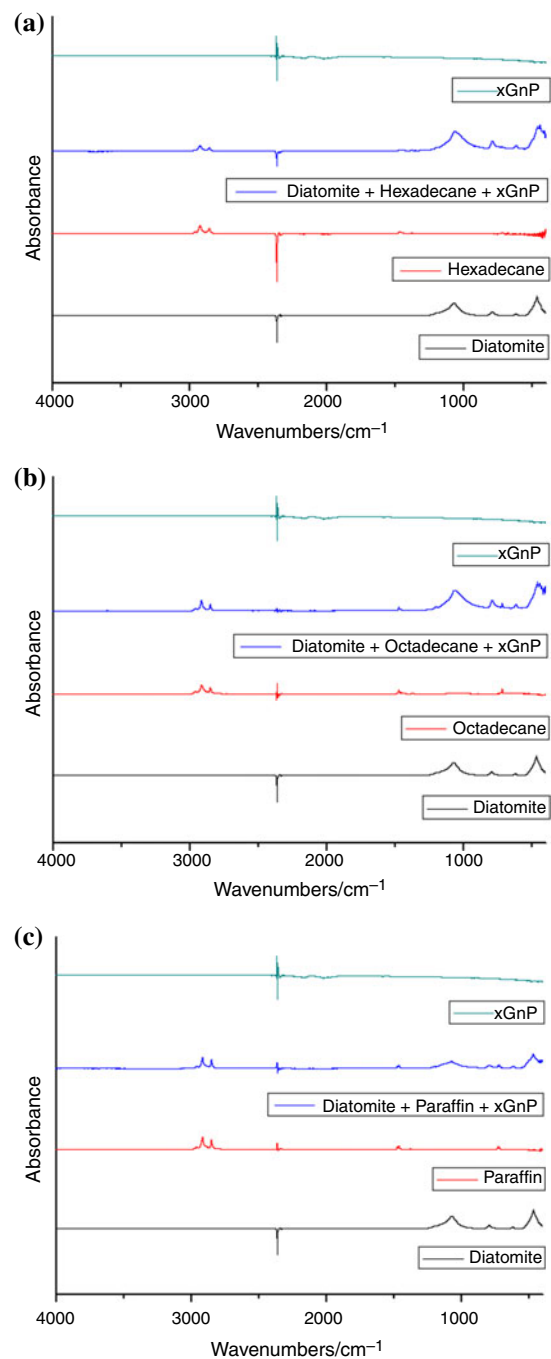


Fig. 3 FTIR analysis of SSPCM + xGnP composites **a** hexadecane + diatomite + xGnP composite, **b** octadecane + diatomite + xGnP composite, and **c** paraffin + diatomite + xGnP composite

xGnP enhanced the thermal resistance of SSPCM. Also, the mass loss of SSPCM with xGnP is higher than that of SSPCM without xGnP. That is because the xGnP led to an improvement in the rate of incorporation of PCM, as seen in DSC analysis. From the TG analysis, we determined that the xGnP supplied high thermal resistant properties to the PCM/diatomite composite.

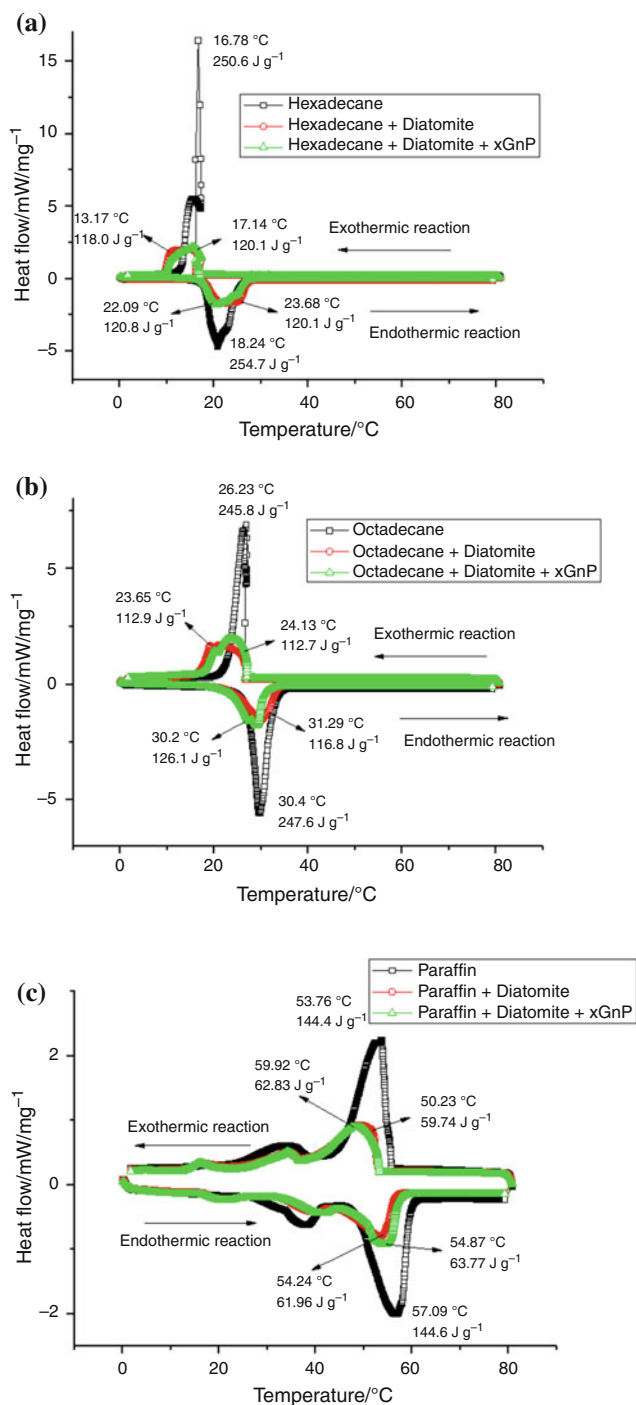


Fig. 4 DSC analysis of SSPCM + xGnP composites **a** hexadecane + diatomite + xGnP composite, **b** octadecane + diatomite + xGnP composite, and **c** paraffin + diatomite + xGnP composite

Thermal conductivity analysis

The thermal conductivity analysis of SSPCM is shown in Fig. 6. Each PCM was approximately 0.32, 0.18, and 0.23 W mK⁻¹ of thermal conductivity in this graph. Also,

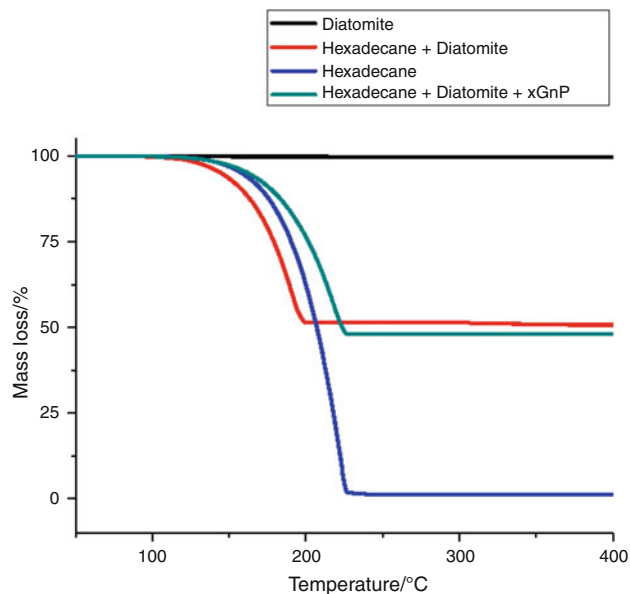


Fig. 5 Thermogravimetry analysis of hexadecane + diatomite + xGnP composite

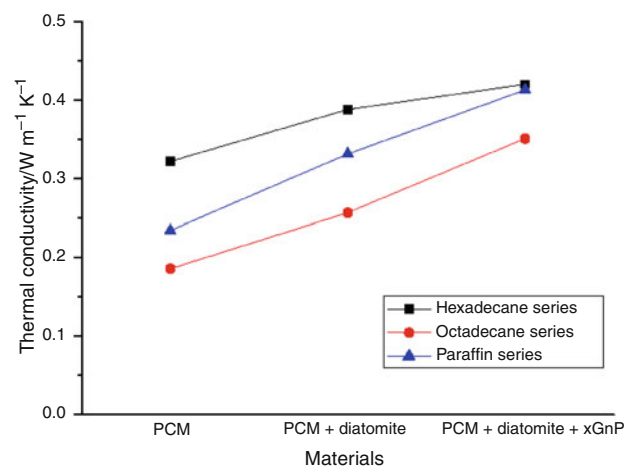


Fig. 6 Thermal conductivity of SSPCM + xGnP composites

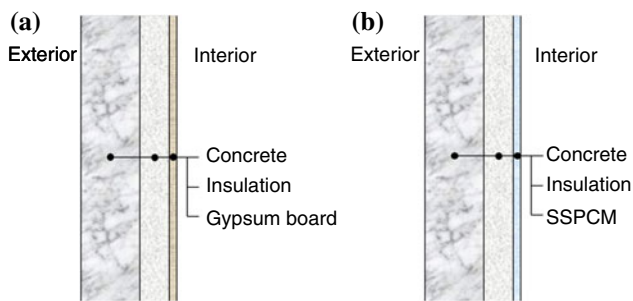
thermal conductivity of the PCM/diatomite composites showed 0.39, 0.25, and 0.33 W mK⁻¹, respectively. It shows that incorporating PCM into the structure of diatomite improves the thermal conductivity of PCMs. However, the rate of increase of thermal conductivity according to the sample is not high. We determined that the SSPCM with xGnP showed 0.42, 0.35, and 0.41 W mK⁻¹. It can be seen that the thermal conductivity of the SSPCM loaded with xGnP improved a little, compared to that of SSPCM without xGnP. The thermal conductivity of the PCM/diatomite/xGnP composites increased by less than 10 %, compared with the SSPCM without xGnP, respectively. Consequently, we analyzed that loading xGnP led to an improvement of the thermal conductivity of SSPCM (Tables 1, 2).

Table 1 DSC analysis of SSPCM with xGnP

PCM Samples	Melting point/°C	Freezing point/°C	Solid–liquid latent heat/J g ⁻¹	Liquid–solid latent heat/J g ⁻¹
Hexadecane + diatomite	23.68	13.17	120.1	118.0
Hexadecane + diatomite + xGnP	22.09	17.14	120.8	120.1
Octadecane + diatomite	31.29	23.65	116.8	112.9
Octadecane + diatomite + xGnP	30.2	24.13	126.1	112.7
Paraffin + diatomite	54.24	50.23	61.96	59.74
Paraffin + diatomite + xGnP	54.87	49.92	63.77	62.83

Table 2 Thermal conductivity of PCM, SSPCM, and SSPCM with xGnP

PCM Samples	Hexadecane group/W m ⁻¹ K ⁻¹	Octadecane group/W m ⁻¹ K ⁻¹	Paraffin group/W m ⁻¹ K ⁻¹
Pure PCM	0.3217	0.1859	0.2342
PCM + diatomite	0.3880	0.2567	0.3312
PCM + diatomite + xGnP	0.4199	0.3510	0.4128

**Fig. 7** Wall section of simulation **a** section without PCM, and **b** section with PCM

Simulation results for application of SSPCMs

Energy Plus is an energy analysis and thermal load simulation program. Based on a user's description of a building, from the perspective of the building's physical make-up and associated mechanical and other systems, Energy Plus calculates the heating and cooling loads necessary to maintain thermal control set points, conditions throughout a

Table 4 Physical properties of SSPCM

Physical properties	Hexadecane-based SSPCM
Melting point/ °C	18.24
Conductivity/W m ⁻¹ K ⁻¹	0.42
Density/kg m ⁻³	777
Specific heat/J kg ⁻¹ K ⁻¹	39,066
Latent heat/J g ⁻¹	120
Thickness/m	0.0125

secondary HVAC system and coil loads, and the energy consumption of primary plant equipment. Energy Plus models heating, cooling, lighting, ventilation, other energy flows, and water use. Energy Plus includes many innovative simulation capabilities: time-steps of less than an hour, modular systems and plant integrated with heat balance-based zone simulation, multi-zone air flow, thermal comfort, water use, natural ventilation, and photovoltaic systems. The dimensions of the simulated room are 4 m (width) × 3 m (depth) × 3 m (height). The weather data for Seoul in EPW

Table 3 Material properties and U-value of exterior wall

Exterior wall without PCM			Exterior wall with PCM		
Material	Thermal conductivity/W m ⁻¹ K ⁻¹	Thickness/m	Material	Thermal conductivity/W m ⁻¹ K ⁻¹	Thickness/m
Concrete	2.000	0.2	Concrete	2.000	0.2
Insulation	0.035	0.1	Insulation	0.035	0.1
Gypsum board	0.18	0.0125	SSPCM	0.42	0.0125
U-value	0.313		U-value	0.317	

format were obtained from Real-Time Weather Data at EERE (Energy Efficiency & Renewable Energy). A PCM layer was assumed to be installed on the insulation of a four-sided exterior wall. Figure 7 shows (a) the section without PCM, and (b) the section with PCM. Table 3 shows the material properties and U-value of the exterior wall. The material properties were referred to ASHRAE Handbook Fundamentals 2,009. The heat that has been generated enters the material through the sensor, during which a voltage

decrease occurs rapidly at the heating source, and the thermal conductivity is calculated through the voltage decrease data. Table 4 shows the overall properties of each PCM, which were measured as mentioned above. The dimensions of the simulated room are 4 m (width) \times 3 m (depth) \times 3 m (height). The weather data for Seoul in EPW format were obtained from Real-Time Weather Data at EERE (Energy Efficiency & Renewable Energy). The measured outdoor temperature was recorded to be the data source for

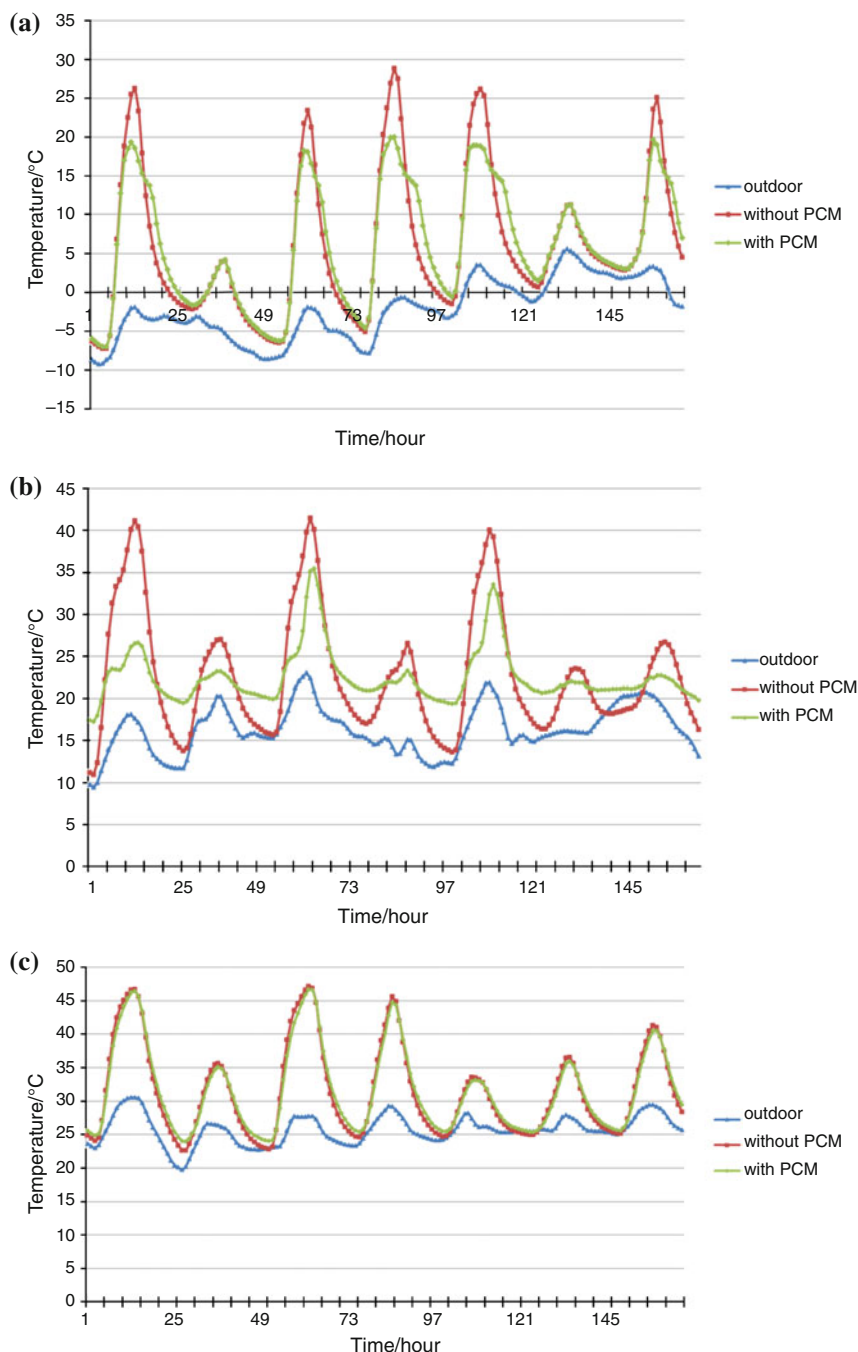


Fig. 8 Simulated results of the indoor temperature during simulated period

simulating the simulated room. Figure 8a, b shows the measured and simulated results of the indoor air temperature, during January and May 1–7. It is seen that the agreement is satisfactory. The figure shows that, in the times of day during which the outside temperature is the lowest, the PCM supplies stored energy to the environment. Therefore, the increase of indoor temperature reaches values between 0 and 6 °C over the indoor temperature without PCM. The measured outdoor temperature was recorded to be the data source for simulating the simulated room. Figure 8c shows the measured and simulated results of the indoor air temperature, during August 1–7. However, it is seen that the agreement is unsatisfactory. It shows that PCM has remained as the liquid state in the summer season because the melting point of PCM is lower than the average temperature of summer season. Taking into consideration the analysis of the result, it can be inferred that PCMs are also efficient accumulators in the summer season. In this case, it will be necessary to raise the nominal temperature of the phase change, in order to make the system work more effectively as a heat sink. Also, we carried out simulation of the SSPCM containing xGnP. The result of this simulation is similar to the simulation of SSPCM. It means that the low enhanced thermal conductivity of the sample did have not an effect on the simulation.

Conclusions

Due to global warming, the need for energy conservation has become critical. To solve this problem, resident buildings must be designed to reduce energy consumption, and control indoor temperature automatically. The application of PCM as a building material will contribute to solving this problem. PCMs can be used to improve thermal performances of building fabrics, and help moderate indoor temperature variations. In Korea, radiant floor heating systems, which have traditionally been used in residential buildings, have a substantially different temperature distribution from buildings using other heating systems because the hot water pipe heating medium is installed under the finishing materials, leading to a significant difference of vertical indoor air temperature. Therefore, the melting point of PCMs suitable for temperature distribution of residential buildings using radiant floor heating systems should be considered, to optimize the PCM performance. Therefore, we prepared PCM/diatomite/xGnP composites for the reduction of energy saving, and enhancement of thermal conductivity. The SSPCM/xGnP composites were prepared by vacuum impregnation, and we determined the characteristics of SSPCM with xGnP by SEM, FTIR, DSC, TG, TCI, and energy simulation analyses. The xGnP was completely dispersed into the SSPCM, and the whole material was incorporated by mechanical bonding. Also, the containing xGnP of the SSPCM did not influence the

decrease of latent heat storage of the SSPCM. We found that the high thermally resistant properties of diatomite and xGnP led to enhance the thermal resistance of the SSPCM with xGnP. Also, xGnP enhanced the thermal conductivity of the sample. The measured and simulated results of the indoor air temperature during January 1–7 and May 1–7 demonstrate a satisfactory agreement. On the other hand, the measured and simulated indoor air temperature during August 1–7 show an unsatisfactory agreement. Taking into consideration the analysis of the result, it can be inferred that they are also efficient accumulators in the summer season. In this case, it will be necessary to raise the nominal temperature of the phase change, in order to make the system work more effectively as a heat sink.

Acknowledgments This study was supported by the National Research Foundation of Korea (NRF) grant funded by the Korea government (MEST) (No. 2012-0005188). This study is financially supported by the Advanced Track of Green Production Processing for Reducing Greenhouse Gas Emission of the KETEP grant funded by Ministry of Knowledge Economy (NO. 20114010203140).

References

1. Cai Y, Wei Q, Huang F, Gao W. Preparation and properties studies of halogen-free flame retardant form-stable phase change materials based on paraffin/high density polyethylene composites. *Appl Energy*. 2008;85:765–75.
2. Veerappan M, Kalaiselvam S, Iniyan S, Goic R. Phase change characteristic study of spherical PCMs in solar energy storage. *Sol Energy*. 2009;83:1245–52.
3. Kim S, Drzal LT. High latent heat storage and high thermal conductive phase change materials using exfoliated graphite nanoplatelets. *Sol Energy Mater Sol Cells*. 2009;93:136–42.
4. Cai Y, Wei Q, Huang F, Lin S, Chen F, Gao W. Thermal stability, latent heat and flame retardant properties of the thermal energy storage phase change materials based on paraffin/high density polyethylene composites. *Renew Energy*. 2009;34:2117–23.
5. Xu X, Zhang Y, Lin K, Di H, Yang R. Modeling and simulation on the thermal performance of shape-stabilized phase change material floor used in passive solar buildings. *Energy Build*. 2005;37:1084–91.
6. Lin K, Zhang Y, Xu X, Di H, Yang R, Qin P. Experimental study of under-floor electric heating system with shape-stabilized PCM plates. *Energy Build*. 2005;37:215–20.
7. Zhang YP, Lin KP, Yang R, Di HF, Jiang Y. Preparation, thermal performance and application of shape-stabilized PCM in energy efficient buildings. *Energy Build*. 2006;38:1262–9.
8. Cheng W, Zhang R, Xie K, Liu N, Wang J. Heat conduction enhanced shape-stabilized paraffin/HDPE composite PCMs by graphite addition: preparation and thermal properties. *Sol Energy Mater Sol Cells*. 2010;94:1636–42.
9. Alkan C, Sari A, Karaipekli A. Preparation, thermal properties and thermal reliability of microencapsulated n-eicosane as novel phase change material for thermal energy storage. *Energy Convers Manage*. 2011;52:687–92.
10. Davis L. Diatomite. *Am Ceram Soc Bull*. 1991;70:860–1.
11. He B, Setterwall F. Technical grade paraffin waxes as phase change materials for cool thermal storage and cool storage systems capital cost estimation. *Energy Convers Manage*. 2002;43:1709–23.

12. Zhang Z, Fang X. Study on paraffin/expanded graphite composite phase change thermal energy storage material. *Energy Convers Manage.* 2006;47:303–10.
13. Stritih U. Heat transfer enhancement in latent heat thermal storage system for buildings. *Energy Build.* 2003;35:1097–104.
14. Frusteri F, Leonardi V, Vasta S, Restuccia G. Thermal conductivity measurement of a PCM based storage system containing carbon fibers. *Appl Therm Eng.* 2005;25:1623–33.
15. Nakaso K, Teshima H, Yoshimura A, Nogami S, Hamada Y, Fukai J. Extension of heat transfer area using carbon fiber cloths in latent heat thermal energy storage tanks. *Chem Eng Process.* 2008;47:879–85.
16. Zeng JL, Cao Z, Yang DW, Xu SunLX, Zhang LF, Zhang L. Effects of MWNTs on phase change enthalpy and thermal conductivity of a solid–liquid organic PCM. *J Therm Anal Calorim.* 2009;95:507–12.
17. Zeng JL, Liu YY, Cao ZX, Zhang J, Zhang ZH, Sun LX, Xu F. Thermal conductivity enhancement of MWNTs on the PANI/tetradecanol form-stable PCM. *J Therm Anal Calorim.* 2008;91:443–6.
18. Xiao M, Feng B, Gong K. Preparation and performance of shape stabilized phase change thermal storage materials with high thermal conductivity. *Energy Convers Manage.* 2002;43:103–8.
19. Py X, Olives R, Mauran S. Paraffin/porous-graphite-matrix composite as a high and constant power thermal storage material. *Int J Heat Mass Transf.* 2001;44:2727–37.
20. Mills A, Farid M, Selman JR, Al-Hallaj S. Thermal conductivity enhancement of phase change materials using a graphite matrix. *Appl Therm Eng.* 2006;26:1652–61.
21. Zeng JL, Cao Z, Yang DW, Sun LX, Zhang L. Thermal conductivity enhancement of Ag nanowires on an organic phase change material. *J Therm Anal Calorim.* 2010;101:385–9.
22. Jeon J, Jeong S, Lee J, Seo J, Kim S. High thermal performance composite PCMs loading xGnP for application to building using radiant floor heating system. *Sol Energy Mater Sol Cells.* 2012;101:51–6.
23. Zhang D, Zhou J, Wu K, Li Z. Granular phase changing composites for thermal energy storage. *Sol Energy.* 2005;78:471–80.
24. Fang X, Zhang Z, Chen Z. Study on preparation of montmorillonite-based composite phase change materials and their applications in thermal storage building materials. *Energy Convers Manage.* 2008;49:718–23.
25. Kim H, Lee B, Choi S, Kim S, Kim H. The effect of types of maleic anhydride-grafted polypropylene (MAPP) on the interfacial adhesion properties of bio-flour-filled polypropylene composites. *Compos A.* 2007;38:1473–82.
26. Jeong S, Jeon J, Seo J, Lee J, Kim S. Performance evaluation of the microencapsulated PCM for wood-based flooring application. *Energy Convers Manage.* 2012;64:516–21.
27. Cha J, Seo J, Kim S. Building materials thermal conductivity measurement and correlation with heat flow meter, laser flash analysis and TCi. *J Therm Anal Calorim.* 2012;109:295–300.
28. Fang G, Li H, Yang F, Liu X, Wu S. Preparation and characterization of nano-encapsulated n-tetradecane as phase change material for thermal energy storage. *Chem Eng J.* 2009;153:217–21.